

## Characterization of the Alteration of Debitus *Grisailles*

Carla Machado<sup>1,2\*</sup>, Márcia Vilarigues<sup>1,2</sup> and Teresa Palomar<sup>3</sup>

<sup>1</sup>Department of Conservation and Restoration, Faculty of Science and Technology, NOVA University of Lisbon, Caparica, Portugal;

<sup>2</sup>Research Unit VICARTE – Glass and Ceramics for the Arts, Faculty of Science and Technology, NOVA University of Lisbon, Caparica, Portugal;

<sup>3</sup>Institute of Ceramic and Glass, Spanish National Research Council (ICV-CSIC), Madrid, Spain

\*Corresponding author: [cf.machado@campus.fct.unl.pt](mailto:cf.machado@campus.fct.unl.pt) (C.Machado)

### Abstract

Stained glass restoration generally involves filling glass losses to maintain the coherence of the window and the new glasses used to fill the losses can be painted to chromatically reintegrate the stained-glass panel. One of the most common painting materials on stained glass is grisaille, a paint made by mixing metal oxides with a ground lead glass. Grisailles usually have black and brown hues and are used for the creation of outlines as shadows in window glasses. Although several commercial companies sell many types of products to paint on glass, few of them present the necessary compatibility with the original materials that conservation materials must have. Debitus is one of the most renowned companies, and its grisailles are frequently used for chromatic reintegration in stained glass window restoration. Thus, the main objective of this study was to assess the long-term stability and durability of commercial Debitus grisailles. Two alteration tests were carried out, with samples placed in high humidity chambers and submerged in distilled water. The samples and degradation products were characterized by optical microscopy,  $\mu$ -Raman spectroscopy, and colourimetry. In the immersion, the pH of the water was measured during the experiment, and the leached elements were analyzed at the end by inductively coupled plasma atomic emission spectroscopy. The results showed an alteration of the colour and the formation of degradation products, identified as sulphates. The solution pH was increased by the aqueous extraction of alkaline and alkaline-earth ions from the support glass of the samples. Despite these changes, it was possible to conclude that these commercial grisailles presented good durability and stability for use in conservation treatments.

### Keywords

Debitus; grisaille; stained-glass window; degradation; conservation

Published in the *Studies and Conservation* journal (2022), 67:7, 413-422.

<https://doi.org/10.1080/00393630.2021.1890965>

It is deposited under the terms of the Creative Commons Attribution-NonCommercial License (<http://creativecommons.org/licenses/by-nc/4.0/>), which permits non-commercial re-use, distribution, and reproduction in any medium, provided the original work is properly cited.

## Introduction

Grisaille is the first paint to be applied in the production of stained-glass panels. It normally has a dark colour and is used for the creation of outlines (grisaille à contourner) and shadows (grisaille à modeler), as shown in Figure 1 (Schalm 2000; Machado et al. 2019b). Grisailles are glass-based paints produced by mixing metal oxides, usually iron and/or copper, with a ground high-lead glass. The mixture is blended with a vehicle such as vinegar or water, which will make it suitable for painting, and gum arabic as a temporary binding agent. After being fired at temperatures around 650-700°C, a thin layer of colourless glass with the metal oxides embedded is formed on the surface of the glass panel (Schalm 2000; Machado et al. 2019b).



**Figure 1.** Stained glass PNP2861 – Heraldic panel with Knights, Switzerland, seventeenth century (?) – National Palace of Pena, Portugal. © Parques de Sintra – Monte da Lua.

Glass painters produced the grisailles directly in stained glass workshops and only in the nineteenth century was his industrially prepared and commercially available. One of the first companies to sell grisailles was Lacroix & Cie, established in Paris in 1855 (Schalm, Janssens, and Caen 2003; Machado et al. 2019a). The industrial fabrication led to a separation between the producers and the users, resulting in conservation problems that still persist, such as incompatibility between the painting materials and the glass panels that can lead to the detachment of the painted layers (Machado et al. 2019a, 2019b). At the end of the twentieth century, after Lacroix & Cie stopped the commercialization of these products, the French Section of the International Institute for Conservation (IIC) in partnership with the Laboratoire de Recherche des Monuments Historiques (LRMH), created new formulations of grisailles to be used in conservation and restoration work. This research was trusted to Hervé Debitus, a conservator and specialist in glass painting (Schalm, Janssens, and Caen 2003; Debitus 2014).

In 1991, H. Debitus published the paper “Recherche pour une formulation nouvelle de grisailles”, where a new formulation for grisailles was introduced, based on medieval manuscripts and manufacturer documents from Lacroix & Cie (Debitus 1991; Machado et al. 2019a). In the paper, he described the ideal characteristics for the paints, such as the preservation of colour in the long term, transparency, and a diverse palette for the new range of colours used in nineteenth-century stained-glass windows. Grisailles must also be able to be mixed, allow a good adhesion to the glass support, and have a firing temperature range sufficient to withstand inaccuracies of kilns and different support glasses. Finally, the composition must be well defined to allow reproduction (Debitus 1991).

H. Debitus designed a new collection of grisailles with a common base glass formulation (5 SiO<sub>2</sub>: 4 PbO). Regarding the metal oxides, he indicated that they should have a mineral origin, such as iron oxides for the different hues between the red and black, cobalt oxide calcined with aluminium for the blue, lead antimonates for yellow, tin oxide for white, and chromium oxide for green (Debitus 1991). Some of the

grisailles (Brun XIII, Brun XVI, and Sanguine) were also obtained by using a mixture of the previously prepared ones.

Some years after the publication, Debitus grisailles became commercially available, and they are still sold today. They are one of the most used brands of grisailles in contemporary art and for restoration work on stained glass windows, mainly for the chromatic reintegration during the process of filling losses, as shown in Figure 2. These materials have to be stable, durable, and compatible with historical windows to avoid future conservation problems.



**Figure 2.** Example of a restored panel using Debitus grisailles. Rondel D4 from the panel *Bandeira de Porta/Janela*, sixteenth/seventeenth century, National Palace of Ajuda, Portugal. © Ângela Santos and Sara Louro.

Today, due to patent protection, the information given by the Debitus company is limited. For example, it is just said that grisailles are made by a mixture of 'Rocaille' ( $5 \text{ SiO}_2: 4 \text{ PbO}$ ) with metal oxides as colourants, with no specific information regarding the metals responsible for each colour or their proportions (Debitus 2014). A previous study characterized five of the most common Debitus grisailles (Machado et al. 2019a). A change was observed between their theoretical composition and the one sold today by the company (Machado et al. 2019a). New elements are now added to the mixture, such as manganese in the *Noir Ordinaire* grisaille, and tin and aluminium in the *Depoli incolore* grisaille, with the function of colouring agent and opacifier, respectively (Machado et al. 2019a).

Although historical grisailles used to be heterogeneous (Marschner 1996; Verità 1996; Schalm, Janssens, and Caen 2003; Verità, Nicola, and Sommariva 2003; Vilarigues and Da Silva 2004; Carmona, Villegas, and Navarro 2006; Pradell et al. 2016), Debitus grisailles are very homogeneous, with good dispersion of the metal grains in the base-glass matrix (Machado et al. 2019a). This homogeneity may be linked to the industrialization process of grinding and mixing. The study also showed that grisailles presented a smooth interface to the glass support, suggesting good interdiffusion and penetration of the grisaille into the glass, as well as good adhesion between the painted layer and the glass substrate (Machado et al. 2019a).

These paints are good-quality materials, appropriate for use in conservation and restoration work. However, one of the most common causes of alteration on grisailles is environmental moisture, which seeps in through fissures leading to the dealkalinization of the underlying glass and loss of adhesion to the glass substrate. External factors such as rain, aerosols, and pollution can also accelerate the degradation rate due to the formation of new crystalline materials on the surface or inside bubbles which promote the powdering of the paint layer (Bettembourg 1991; Perez y Jorba 1991; Verità 1996; Schalm, Janssens, and Caen 2003; Verità, Nicola, and Sommariva 2003; Verità 2010; Palomar 2018). Therefore, to evaluate the future of these commercial grisailles, further studies needed to be done to assess their behaviour in the long term and the effect of ageing on them. For this reason, the main objective of this work was to assess the morphological and chemical durability and stability of these commercial grisailles in common aggressive environments.

## Methodology

### Materials and methods

Five grisailles (Noir Ordinaire, Brun XIII, Brun XVI, Mousseline, and Depoli Incolore), characterized in a previous study (Machado et al. 2019a), were chosen for this study. This choice allowed a comparison between the results obtained and the ones previously published.

Two alteration tests were carried out: 1) exposure in high-humidity chambers (at 95% and 80% RH) permanently sealed at environmental temperature for 30 months; 2) immersion in stable conditions in distilled water for three months. For all grisailles three replicates of each were subjected to the different aging tests. Figure 3 shows a schematic representation of the distribution of the samples in the alteration tests.

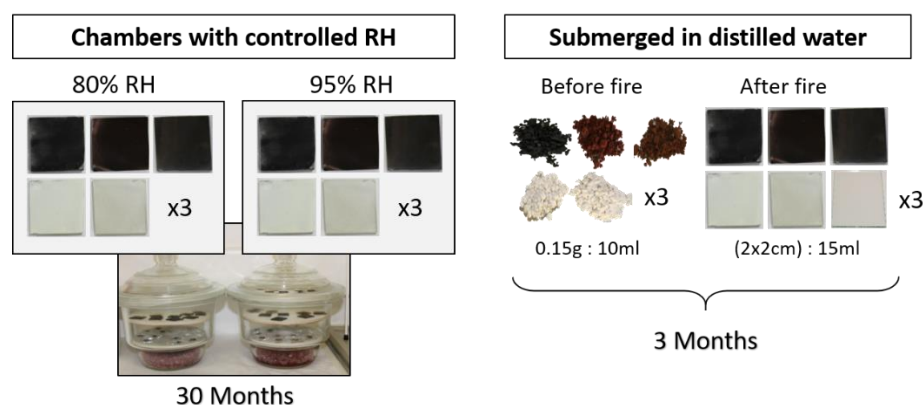


**Figure 3.** Schematic representation of the alteration regimes.

The alteration tests were made on grisailles powder before being fired and painted samples after being fired. Painted grisailles were prepared with a mixture of water and gum arabic (less than 1 wt. %) and painted on  $2 \times 2$  cm squares on flat soda-lime glasses. Only one glass composition was chosen to better control the study variables, as the support can influence the grisaille degradation (Perez y Jorba 1991; Vilarigues et al. 2020). This glass was chosen for its stability and because it is the most common glass composition used for glass-fills paint with grisaille in stained glass window restoration.

The painted samples were fired in a side-heated electric furnace (BARRACHA-Model E1) with a temperature ramp of  $3 \text{ }^\circ\text{C}/\text{min}$  up to  $680 \text{ }^\circ\text{C}$ , followed by a dwell of 30 min and slow cooling. A fifth set was stored in normal environmental conditions for comparison.

### Analytical techniques

The samples before and after the alteration tests were also chemically, morphologically, and chromatically characterized by X-ray fluorescence (XRF), optical microscopy (OM),  $\mu$ -Raman spectroscopy, and colourimetry and particle size distribution was calculated using laser diffraction. The pH of the aqueous solution from the alteration tests was measured and analyzed by inductively coupled plasma atomic emission spectroscopy (ICP-AES).

To identify the chemical composition of the grisailles studied, by XRF, a PANalytical MagicX (PW-2424) wavelength dispersive X-ray spectrometer equipped with a rhodium tube (SUPER SHARP) of 2.4 KW was used. Analytical determinations were carried out through the analysis curve, with a powder sample prepared in a fused pearl. The pearls were made in a Philips PerI'X3 equipment being melted at  $1050 \text{ }^\circ\text{C}$ , in a platinum-gold crucible, from a homogeneous mixture of 0.3 g of the powder sample ( $< 75 \text{ }\mu\text{m}$ ) and 5.5 g of  $\text{Li}_2\text{B}_4\text{O}_7$  anhydro and LiBr.

The particle size of the powders before the firing process was calculated by laser diffraction in a Mastersizer S from Malvern Instruments Ltd. (UK) using an aqueous suspension of the solid with three

drops of Dolapix CE-64 1/100 as a dispersant and applying ultrasound for 5 min to disperse and stabilize the particles.

OM was used to characterise the particle morphology of the samples before the alteration tests as well as the alteration and the formation of degradation products after the tests. The samples were also observed in cross-sections; after cutting the samples, they were embedded in Araldite® 2020 resin and polished to optical quality. The microscope used was an Axioplan 2 from Zeiss, equipped with a halogen light HAL100 and digital camera (Nikon DMX1200F).

For the characterization of the colouring agents and the degradation products,  $\mu$ -Raman spectroscopy was used. The spectrometer, a LabRaman 300 Jobin Yvon, is equipped with a 17 mW HeNe laser operating at 632.8 nm. The laser beam was focused with a 50x Olympus objective lens. When needed, the laser power was controlled using neutral density filters 0.3 and 0.6, with a collection time of 10 s performing 15 scans.

A colorimetric study was done using ultraviolet—visible spectroscopy (UV-VIS) to observe alterations in the colour of the samples. The fibre optic spectrometer used was an Avantes AvaSpec-2048, with a 300 lines/mm grating, and a wavelength range of 200-1100 nm. The analyses were done with an integrating sphere (AVASPHERE-50-REFL) and 600  $\mu$ m reflection probe (Avantes FC-UV600-2) in three different areas of each sample, and an average of the results was calculated. The change in lightness  $\Delta L^*$  (Eq.1) and colour difference  $\Delta E^*$  (Eq.2) were also calculated, to see the difference between the original and altered samples.

$$\Delta L^* = \Delta L^*_{(\text{altered})} - \Delta L^*_{(\text{original})} \quad (\text{Eq.1})$$

$$\Delta E^* = \sqrt{\Delta L^2 + \Delta a^2 + \Delta b^2} \quad (\text{Eq.2})$$

The pH of the aqueous solution was also measured for three months. The equipment used was a Sartorius Docu pH meter, using an electrode with a KCl 3M solution.

At the end of the alteration tests, the aqueous solutions were analyzed by ICP-AES to quantify the compounds leached from the samples after long-term contact with water. A Horiba Jobin–Yvon Ultima model was used, equipped with a 40.68 MHz RF generator, Czerny-Turner monochromator with 1.00 m (sequential), and an AS500 autosampler.

## Results and discussion

### Grisailles characterization

The XRF results shown in Table 1 indicated that iron, zinc, and manganese oxides were used as colouring agents in the darker grisailles and tin oxide in the clear ones. The base glass was identified as high-lead silica glass with a PbO/SiO<sub>2</sub> ratio between 44 - 46 mol. % and, despite the small difference, it appears that the same glass was used for the production of the different grisailles (Machado et al. 2019a). These results showed an agreement with the compositions described in the literature for the Debitus grisailles now in commercial use today (Machado et al. 2019a).

High-lead silica glass, as was used in the production of these grisailles, usually has good chemical stability; however, in stained glass windows, it is susceptible to the action of rain or condensation. It is a slow reaction, and external protective glazing usually prevents it (Verità 2010).

The proportion between the base glass (BG) and the colouring agents (CA), calculated in Table 1, is suitable for fixing the paint to the glass support and coating the glass substrate effectively. When the proportion of colouring agents is higher, it can lead to a more porous grisaille which is more susceptible to abrasion moisture and atmospheric agents of deterioration (Bettembourg 1991). The obtained results agree with the proportions found in the literature for more recent grisailles (nineteenth and twentieth century) that showed good diffusion into the glass support (Palomar 2013; Pradell et al. 2016). Thus, the studied

grisailles will have good adhesion between the painted layer and the glass substrate, improving their long-term conservation.

**Table 1.** Chemical composition from the grisaille samples obtained by XRF. Relations between PbO and SiO<sub>2</sub>\* and between the base glass (BG) and the colouring agents (CA)\*\*.

		Al <sub>2</sub> O <sub>3</sub>	SiO <sub>2</sub>	K <sub>2</sub> O	MnO	Fe <sub>2</sub> O <sub>3</sub>	ZnO	SnO <sub>2</sub>	PbO	PbO/SiO <sub>2</sub> *	BG/CA**
<b>Brun XIII</b>	<b>wt.%</b>	0.52	16.2	0.16	2.17	24.8	4.57	-	51.6	-	-
	<b>mol. %</b>	0.68	35.97	0.23	4.08	20.72	7.49	-	30.84	46.16	67.42
<b>Brun XVI</b>	<b>wt.%</b>	0.47	16.7	-	2.53	23.65	4.57	-	49.5	-	-
	<b>mol. %</b>	0.62	37.35	-	4.79	19.90	7.55	-	29.80	44.38	67.56
<b>Noir ordinaire</b>	<b>wt.%</b>	0.78	18.1	0.19	6.40	21.3	0.04	-	53.2	-	-
	<b>mol. %</b>	0.99	38.95	0.26	11.67	17.25	0.06	-	30.82	44.17	70.66
<b>Depoli Incolore</b>	<b>wt.%</b>	8.5	20.8	-	-	-	-	5.34	65.4	-	-
	<b>mol. %</b>	11	45.67	-	-	-	-	4.67	38.66	45.84	94.75
<b>Mousseline</b>	<b>wt.%</b>	0.28	16.5	-	-	-	-	34.0	49.3	-	-
	<b>mol. %</b>	0.38	37.94	-	-	-	-	31.17	30.51	44.58	68.71

\*PbO/SiO<sub>2</sub> = PbO/(PbO+SiO<sub>2</sub>) \*\*BG/CA = PbO+SiO<sub>2</sub>/((PbO+SiO<sub>2</sub>)+MnO+Fe<sub>2</sub>O<sub>3</sub>+ZnO) or = PbO+SiO<sub>2</sub>/((PbO+SiO<sub>2</sub>)+SnO<sub>2</sub>)

The particle size distribution results, represented in Figure 4, showed that both the darker and the clear grisailles have the same particle size range (ø 0.15–40.00 µm), which can be related to the industrialization process for grinding the mixtures. The sizes are distributed in two different groups, probably related to the two compounds in grisailles: the colouring agents and the high-lead glass.

In both samples, the smallest group (ø 0.15–3.00 µm) is the one with less percentage volume. Comparing these results with the chemical composition presented in Table 1, the colouring agents (Fe<sub>2</sub>O<sub>3</sub>, SnO, MnO, ZnO) are in lower quantity than the ones used in the base glass (SiO<sub>2</sub>, PbO), so they could correspond to the group of smaller particle size. The larger group (ø 3.00–40.00 µm) with a higher percentage volume could correspond to the base glass particles.

The small particle size of the colouring agents gives greater homogeneity to these grisailles, after being fired, when compared with historical ones (Marschner 1996; Verità 1996). This increases durability because large grains of metal oxides (ø 1.00–30.00 µm) in combination with bubbles and fissures can interrupt the continuity of the glass film, accelerating the degradation process (Bettembourg 1991; Verità 1996; Verità, Nicola, and Sommariva 2003; Vilarigues and Da Silva 2004; Silvestri, Molin, and Pomero 2011; Pradell et al. 2016).

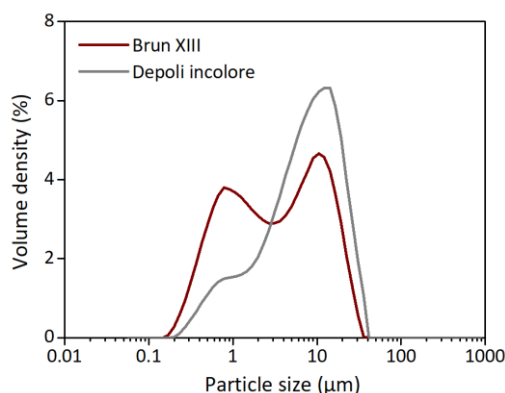


**Figure 4.** Particle size distribution of the Brun XIII and Depoli incolore grisailles before firing.

Table 2 presents the crystallographic phases that were identified in the grisailles after the firing process (Machado et al. 2019a). A mixture of different iron oxides (hematite, magnetite) and kentrolite were

identified in the darker grisailles, as well as a compound with zinc and iron in the Brun XIII and Brun XVI grisailles. In the clear grisailles, only cassiterite (SnO<sub>2</sub>) was found. These crystallographic phases are the compounds that act as colouring agents.

**Table 2.** Crystallographic phases of the grisailles after firing. Results obtained from X-ray diffraction by Machado et al. (2019a).

	Crystallographic phases
<b>Brun XIII</b>	Kentrolite (Pb <sub>2</sub> Mn <sub>2</sub> O <sub>2</sub> (Si <sub>2</sub> O <sub>7</sub> )); Franklinite (ZnFe <sub>2</sub> O <sub>4</sub> ); Hematite (Fe <sub>2</sub> O <sub>3</sub> ); Magnetite (Fe <sub>3</sub> O <sub>4</sub> )
<b>Brun XVI</b>	Kentrolite (Pb <sub>2</sub> Mn <sub>2</sub> O <sub>2</sub> (Si <sub>2</sub> O <sub>7</sub> )); Franklinite (ZnFe <sub>2</sub> O <sub>4</sub> ); Hematite (Fe <sub>2</sub> O <sub>3</sub> ); Magnetite (Fe <sub>3</sub> O <sub>4</sub> )
<b>Noir Ordinaire</b>	Kentrolite (Pb <sub>2</sub> Mn <sub>2</sub> O <sub>2</sub> (Si <sub>2</sub> O <sub>7</sub> ); Hematite (Fe <sub>2</sub> O <sub>3</sub> ); Magnetite (Fe <sub>3</sub> O <sub>4</sub> )
<b>Depoli incolore</b>	Cassiterite (SnO <sub>2</sub> )
<b>Mousseline</b>	Cassiterite (SnO <sub>2</sub> )

The micrographs shown in Figure 5, revealed a higher heterogeneity in the darker samples than in the clear ones. This heterogeneity can be related to the presence of different crystallographic phases (Table 2).

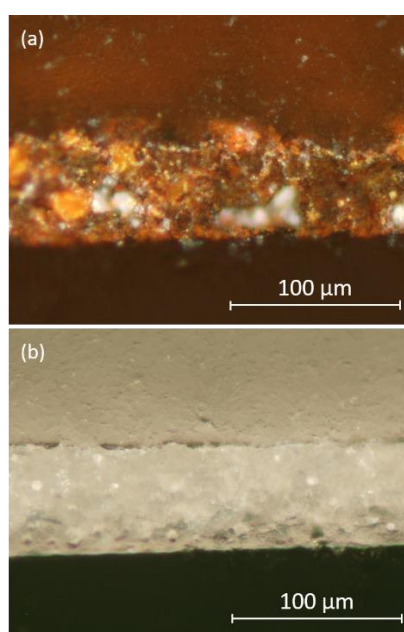


**Figure 5.** Micrographs of Brun XIII (a) and Depoli incolore (b) after firing, in cross-section, in cross-polarized light.

## Grisaille alterations

### Aqueous solution

The pH of the aqueous solution was monitored during the submersion tests, and the solutions were analyzed by ICP-AES at the end of the experiment.

The solution showed an increase in pH, represented in Figure 6, in the beginning, followed by a slight decrease and stabilization after 10 days. Both the powders before being fired and the painted samples showed similar behaviour. This pH increase can be explained by ionic exchange between the alkaline ions from the glass and the hydroxyl (H<sup>+</sup> and H<sub>3</sub>O<sup>+</sup>) from the water (Reaction 1) (Navarro 2003; Machado and Vilarigues 2018).



The pH measurements of the powders before being fired, Figure 6 (a), present an increase of pH ( $\Delta\text{pH} \sim 0.5\text{--}1.5$ ) greater than for the painted samples ( $\Delta\text{pH} < 0.5$ ), due to a higher ratio surface/solution in the powder (Vilarigues and da Silva 2006; Machado and Vilarigues 2018).

Figure 6 (b) shows the comparison of the pH variations between the unpainted glass and the painted samples. This comparison shows that the glass sample has a similar behaviour to the painted samples.

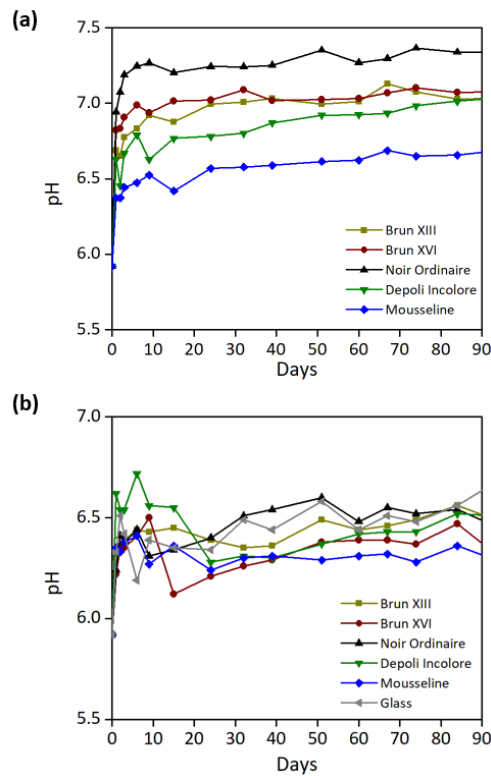


**Figure 6.** pH variation of the aqueous solution with the commercial powder before being fired (a) and with the painted samples (b), after 90 days.

At the end of the immersion period, the aqueous solutions were analyzed by ICP-AES, and the results are shown in Table 3. There was extraction of alkaline and alkaline-earth ions, mainly calcium ( $\text{Ca}^{2+}$ ). As the grisailles do not contain calcium (Table 1), this alkaline-earth ion must come from the glass support.

It is also possible to observe that the darker samples were more leached than the clear ones (Table 3). This can be related to the higher heterogeneity observed in the darker grisailles, as seen in Figure 4, which can favour the formation of bubbles and fissures in the grisaille, allowing the penetration of water. According to these results, the darker grisailles are more susceptible to humidity and in consequence leaching was greater for the painted samples than for the unpainted glass, despite the similar pH variation. Usually, paint layers can protect the glass surface; however, grisaille porosity can facilitate water penetration, favouring localised attack on the glass substrate (Palomar 2018).

**Table 3.** ICP-AES results (mg/l) of the aqueous solution after the experiment.

	Na	Si	Ca	Zn	Sn	Pb
<b>Glass</b>	0.10	0.15	0.14	-	0.02	-
<b>Brun XIII</b>	0.01	-	0.81	-	-	-
<b>Brun XVI</b>	0.09	-	2.25	0.02	-	-
<b>Noir ordinaire</b>	0.09	0.22	2.50	-	-	-
<b>Mousseline</b>	0.01	-	0.61	-	-	0.04
<b>Depoli incolore</b>	-	-	0.27	-	-	0.02

### Alteration pathologies

A greater colour change was observed in the Brun XII and Brun XVI samples compared with the other samples, as is shown in Figure 7 (a). This change is mainly in the grisailles submerged in water, which tend to turn yellow and red.



Hematite ( $\text{Fe}_2\text{O}_3$ ), present in large amounts in these grisailles (Table 2), can react with water after long term contact to form orange-coloured iron oxyhydroxide ( $\text{FeO}(\text{OH})$ ) (Reaction 2) (Lefevre, Duc, and Fédoroff 2006).



Mousseline and Depoli incolore grisailles, the clear ones, showed a similar behaviour (towards red and yellow) but with a smaller colour difference between the original samples and the altered ones, again due to the formation of alteration products. The colour of the Noir ordinaire samples remained almost unchanged.

However, it was in the lightness  $L^*$  that the most significant change was observed for all the grisailles, as shown in Figure 7 (b). This change was mainly seen in the submerged samples as a whitening of the samples, probably related to the formation of degradation products on the surface of the painted layer. The samples submerged in water showed a greater colour change, Figure 7 (c). However, these colour differences are not very significant, relative to the appearance after conservation treatment.

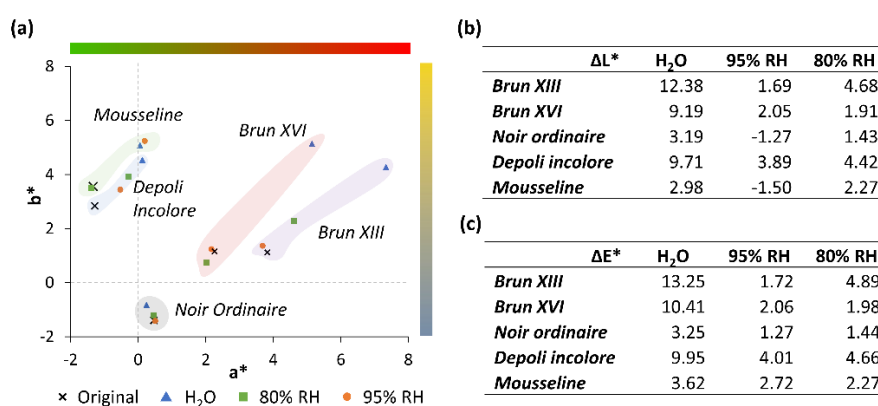


**Figure 7.** Colour measurements  $a^*$  vs  $b^*$  (a),  $\Delta L^*$  (b), and  $\Delta E^*$  (c) after the alteration tests.

Under the optical microscope, it was possible to observe the formation of white crystalline salts, mainly in the samples exposed to the 80% RH chamber, as shown in Figure 8.

To characterize these white crystals as well as the grisaille colouring agents,  $\mu$ -Raman spectroscopy was performed on the surface of the samples, and the results are shown in Figure 9.

In agreement with the X-ray diffraction results from the previous study, shown in Table 2, hematite and cassiterite were observed as the raw materials used in the production of the grisailles and are responsible for the colour. Hematite was identified by the presence of its seven characteristic bands at 225, 247, 291, 410, 497, 611, and  $1320 \text{ cm}^{-1}$  (de Faria, Venâncio Silva, and de Oliveira 1997; Bouchard and Smith 2003; Montagner et al. 2013). Also, the presence of a band at  $660 \text{ cm}^{-1}$ , common in magnetite, can indicate a partial transformation, under the laser beam, of hematite into magnetite (Bouchard and Smith 2003). Cassiterite was identified by the presence of a characteristic strong band at  $633 \text{ cm}^{-1}$  as well as weaker bands at 476 and  $778 \text{ cm}^{-1}$  (Beattie and Gilson 1969; Coentro et al. 2018).

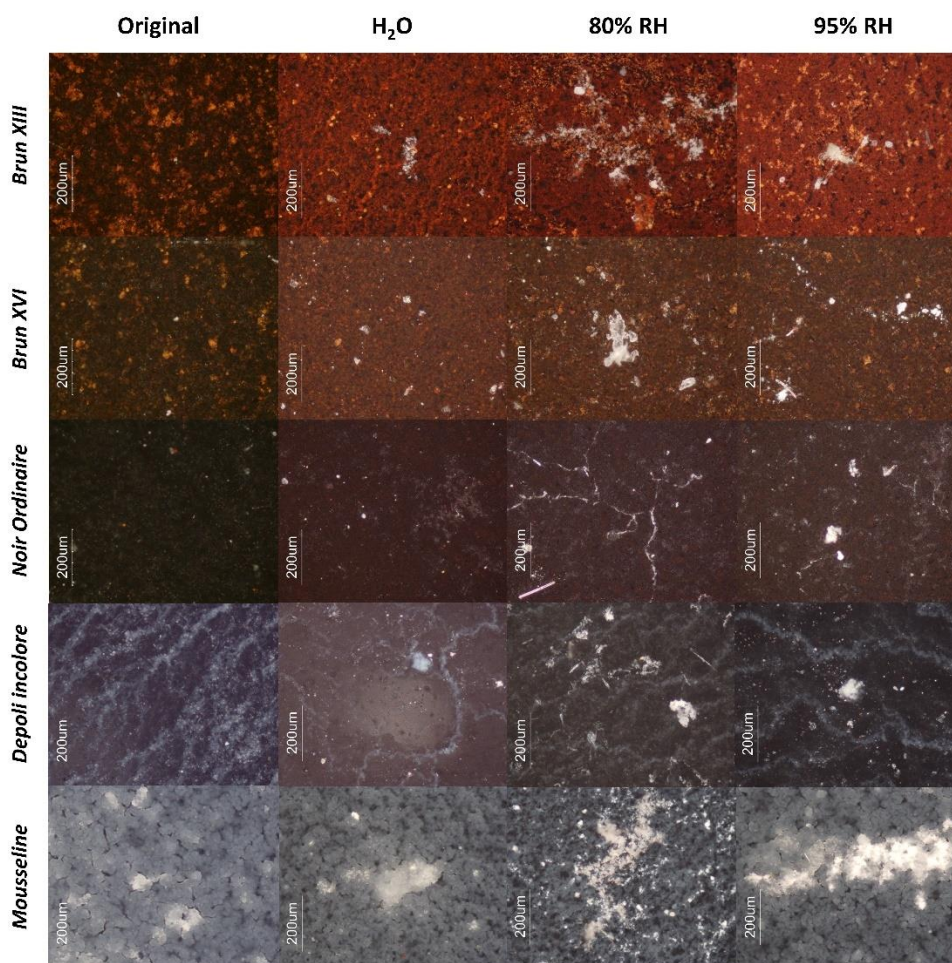


**Figure 8.** Micrographs of the painted samples before and after the alteration tests, viewed with cross-polarized light.

The white crystal deposits formed in the high humidity chambers, observed using the optical microscope, were identified as sodium sulphate ( $\text{Na}_2\text{SO}_4$ ). This identification was made by the presence of a strong peak, as observed in Figure 9, which corresponds to the symmetric stretching vibration from the  $\text{SO}_4^{2-}$  ions, at  $992\text{ cm}^{-1}$ , as well as the presence of a weaker band at  $466\text{ cm}^{-1}$  ( $\nu_2$  bending vibration) and the triplet bands between  $1088\text{--}1188\text{ cm}^{-1}$  ( $\nu_3$  anti-symmetric stretching vibration) (Shantakumari 1953; Sarmiento et al. 2008; Ben Mabrouk et al. 2013; Prieto-Taboada et al. 2019).  $\text{Na}_2\text{SO}_4$  can be formed by the breakdown of the glass network (Reaction 3) and the leaching of  $\text{Na}^+$  ions from the glass support (Reaction 4) that can interact with  $\text{SO}_2$  from the environment to form deposits on the surface (Reaction 5). Although it was not possible to identify carbonates, sulphate formation usually occurs after carbonate formation (Reactions 6 and 7) (Navarro 2003; Vilarigues et al. 2011; Palomar et al. 2017; Palomar 2018; Rodrigues et al. 2018).



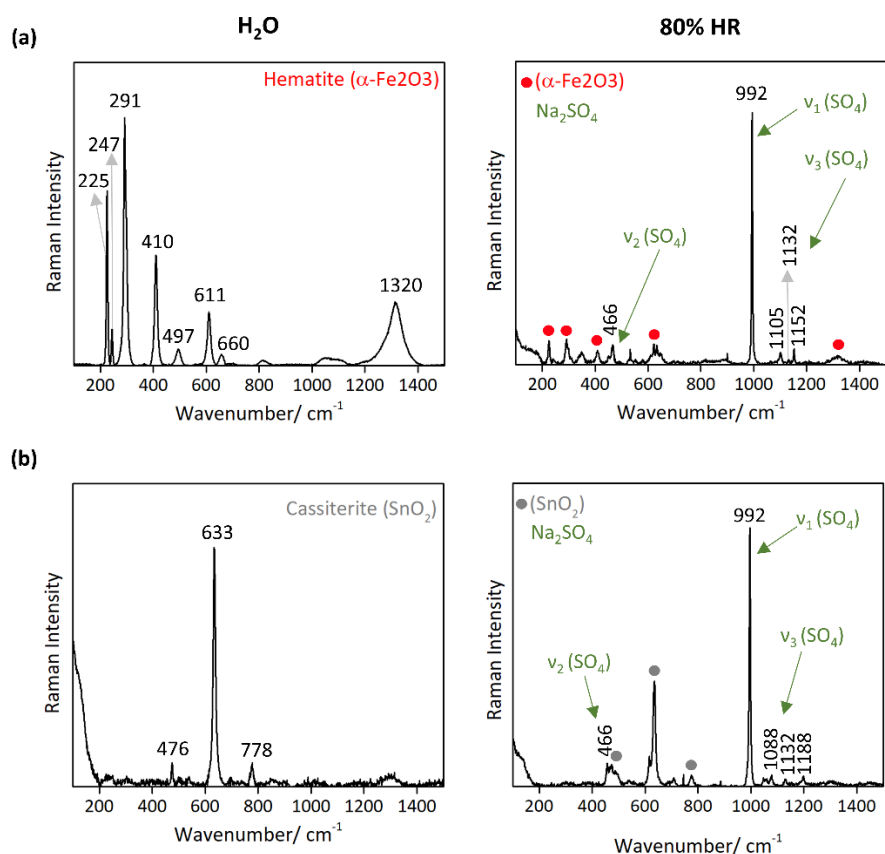


**Figure 9.** Raman spectra of the painted samples Brun XIII (a) and Mousseline (b), submerged in water (left) and from the 80% RH chamber (right).

Both compounds ( $\text{Na}_2\text{CO}_3$ ,  $\text{Na}_2\text{SO}_4$ ) have high solubility, as shown in Table 4, and for this reason, they do not appear in the submerged samples. In the humid atmospheres, it was seen that  $\text{Na}_2\text{SO}_4$  has a slightly lower solubility than sodium carbonate ( $\text{Na}_2\text{CO}_3$ ), having also a lower Gibbs free energy and, therefore, its formation is more favourable. The formation of sodium compounds instead of, for example, more stable calcium compounds can be related to the higher concentration of sodium in the water reacting with the grisaille.

**Table 4.** Solubility at 25 °C and Gibbs free energy of formation in standard conditions (25 °C and 100 kPa) in an aqueous solution of the species. Data obtained from Patnaik (2002), Lide (2005) and Palomar et al. (2017).

Compound	Solubility <sub>25 °C</sub> (g/100 g H <sub>2</sub> O)	$\Delta G_f^\circ$ (kJ·mol <sup>-1</sup> )
$\text{Na}_2\text{CO}_3$	30.7	-1051.6
$\text{Na}_2\text{SO}_4$	28.1	-1268.4
$\text{CaCO}_3$	$6.6 \cdot 10^{-4}$	-1081.4
$\text{CaSO}_4$	0.205	-1298.1
$\text{PbCO}_3$	$1.1 \cdot 10^{-3}$	-625.9
$\text{PbSO}_4$	$4.3 \cdot 10^{-3}$	-813.9
$\text{FeCO}_3$	$6.2 \cdot 10^{-4}$	-666.7
$\text{FeSO}_4$	29.5	-820.8
$\text{Fe}_2(\text{SO}_4)_3$	440	-2242.8
$\text{Fe}_2\text{O}_3$	-	-742.2
$\text{Fe}_3\text{O}_4$	-	-1015.4
$\text{SnSO}_4$	18.8	-
$\text{SnO}_2$	-	-515.8

## Conclusions

This study has provided understanding of the alteration processes of commercial Debitus grisailles. These samples showed small changes of colour and the formation of white crystalline salts, identified as sulphates, on the grisailles' surface after being exposed for a long time to highly humid atmospheres. In addition, the aqueous test showed a small increase in pH. Both the formation of crystalline salts and the increase in pH of the solutions were due to the aqueous extraction of alkaline and alkaline-earth ions from the glass support. This reveals the important influence that the glass support has in the degradation of the grisaille, as well as the influence that the grisailles have, mainly due to their porosity, on the alteration of the glass support.

Despite these observations, Debitus grisailles are stable after firing, and well-fixed to the glass support without any signs of future detachment. Debitus grisailles can be recommended for use in conservation treatments when they are applied to good quality and stable glasses, such as the soda-lime silicate glasses used in this study, and used only on the indoor glass surface to avoid contact with rain. It is recommended that similar studies should be carried out for other commercial brands to evaluate their stability in the long term.

## Data availability

The raw/processed data required to reproduce these findings cannot be shared at this time as the data also form part of an ongoing study.

## Acknowledgements

The authors wish to thank Miguel Gómez (Instituto de Cerámica y Vidrio, CSIC, Madrid) for the particle size measurements and María José Velasco (Instituto de Cerámica y Vidrio, CSIC, Madrid) for the XRF analyses. The authors also wish to acknowledge professional support of the Interdisciplinary Thematic Platform from CSIC Open Heritage: Research and Society (PTI-PAIS).

## Disclosure statement

No potential conflict of interest was reported by the author(s).

## Funding

This work was supported by Fundação para a Ciência e a Tecnologia (Portugal) [Grant Number UID/EAT/00729/2020 and PD/BD/136673/2018]; Fundación General CSIC (Spain) [Grant Number ComFuturo Programme].

## ORCID

Carla Machado <http://orcid.org/0000-0001-8843-1101>

Márcia Vilarigues <http://orcid.org/0000-0003-4134-2819>

Teresa Palomar <http://orcid.org/0000-0002-3762-8788>

## References

- Beattie, I. R., and T. R. Gilson. 1969. "Oxide Phonon Spectra." *Journal of the Chemical Society A: Inorganic, Physical, Theoretical*, 2322–2327. doi:10.1039/j19690002322.
- Ben Mabrouk, K., T. H. Kauffmann, H. Aroui, and M. D. Fontana. 2013. "Raman Study of Cation Effect on Sulfate Vibration Modes in Solid State and in Aqueous Solutions." *Journal of Raman Spectroscopy* 44: 1603–1608. doi:10.1002/jrs.4374.
- Bettembourg, J. M. 1991. "Composition et Durabilité des Grisailles." *Sci. Technol. Conserv. Restaur. Oeuvres Art Patrim* 2: 47–55.

- Bouchard, M., and D. C. Smith. 2003. "Catalogue of 45 Reference Raman Spectra of Minerals Concerning Research in art History or Archaeology, Especially on Corroded Metals and Coloured Glass." *Spectrochimica Acta Part A: Molecular and Biomolecular Spectroscopy* 59: 2247–2266. doi:10.1016/S1386-1425(03)00069-6.
- Carmona, N., M. A. Villegas, and J. M. F. Navarro. 2006. "Study of Glasses with Grisailles from Historic Stained Glass Windows of the Cathedral of León (Spain)." *Applied Surface Science* 252: 5936–5945. doi:10.1016/j.apsusc.2005.08.023.
- Coentro, S., R. C. da Silva, C. Relvas, T. Ferreira, J. Mirão, A. Pleguezuelo, R. Trindade, and V. S. F. Muralha. 2018. "Mineralogical Characterization of Hispano-Moresque Glazes: A  $\mu$ -Raman and Scanning Electron Microscopy with X-Ray Energy Dispersive Spectrometry (SEM-EDS) Study." *Microscopy and Microanalysis* 24: 300–309. doi:10.1017/S1431927618000338.
- de Faria, D. L. A., S. Venâncio Silva, and M. T. de Oliveira. 1997. "Raman Microspectroscopy of Some Iron Oxides and Oxyhydroxides." *Journal of Raman Spectroscopy* 28: 873–878. doi:10.1002/jrs.177
- Debitus, H. 1991. "Recherche Pour une Formulation Nouvelle de Grisailles." *Sci. Technol. Conserv. Restaur. Œuvres Art Patrim* 2: 24–28.
- Debitus, H. 2014. *Paints: Characteristics*. <http://www.debitus.com/peintures-en.php>. Accessed October 24, 2018.
- Lefevre, G., M. Duc, and M. Fédoroff. 2006. "Accuracy in the Determination of Acid-Base Properties of Metal Oxides Surfaces." In *Surf. Complexation Model*, edited by J. Lützenkirchen, 35–66. Karlsruhe (Germany): Elsevier Ltd. doi:10.1016/S1573-4285(06)80046-3
- Lide, D. R., ed. 2005. *CRC Handbook of Chemistry and Physics, Internet Version 2005*. Boca Raton, Florida: CRC Press. <http://www.hbcpnetbase.com>
- Machado, C., A. Machado, T. Palomar, L. C. Alves, and M. Vilarigues. 2019a. "Debitus Grisailles for Stained-Glass Conservation: an Analytical Study." *Conservar Património* 34: 65–72. doi:10.14568/cp2018067.
- Machado, C., A. Machado, T. Palomar, and M. Vilarigues. 2019b. "Grisaille in Historical Written Sources." *Journal of Glass Studies* 61: 71–86.
- Machado, A., and M. Vilarigues. 2018. "Blue Enamel Pigment—Chemical and Morphological Characterization of its Corrosion Process." *Corrosion Science* 139: 235–242. doi:10.1016/j.corsci.2018.05.005.
- Marschner, H. 1996. "Analyses de Pigments de Grisaille sur des Vitraux Munichoises de L'Église du Saint-Sauveur, Réalisés Vers 1500." *Dossier de La Commission Royale Des Monuments, Sites et Fouilles* 3: 53–59.
- Montagner, C., D. Sanches, J. Pedroso, M. J. Melo, and M. Vilarigues. 2013. "Ochres and Earths: Matrix and Chromophores Characterization of 19th and 20th Century Artist Materials." *Spectrochimica Acta Part A: Molecular and Biomolecular Spectroscopy* 103: 409–416. doi:10.1016/j.saa.2012.10.064.
- Navarro, J. 2003. *El Vidrio*. 3rd Editio. Madrid: CSIC Universitarios.
- Palomar, T. 2013. *La interacción de los vidrios hitóricos conmedios atmosféricos, acuáticos e enterramientos*. Universidad Autónoma de Madrid. <http://hdl.handle.net/10486/12962>.
- Palomar, T. 2018. "Chemical Composition and Alteration Processes of Glasses from the Cathedral of León (Spain)." *Boletín de la Sociedad Española de Cerámica y Vidrio* 57: 101–111. doi:10.1016/j.bsecv.2017.10.001.

- Palomar, T., A. Chabas, D. M. Bastidas, D. de la Fuente, and A. Verney-Carron. 2017. "Effect of Marine Aerosols on the Alteration of Silicate Glasses." *Journal of Non-Crystalline Solids* 471: 328–337. doi:10.1016/j.jnoncrysol.2017.06.013.
- Patnaik, P. 2002. *Handbook of Inorganic Chemicals*. New York: The MacGraw-Hill.
- Perez y Jorba, M. 1991. "Composition et Alteration des Grisailles Anciennes." *Sci. Technol. Conserv. Restaur. Oeuvres Art Patrim* 2: 43–45.
- Pradell, T., G. Molina, S. Murcia, R. Ibáñez, C. Liu, J. Molera, and A. Shortland. 2016. "Materials, Techniques and Conservation of Historic Stained Glass "Grisailles,"." *International Journal of Applied Glass Science* 7: 41–58. doi:10.1111/ijag.12125.
- Prieto-Taboada, N., S. Fdez-Ortiz de Vallejuelo, M. Veneranda, E. Lama, K. Castro, G. Arana, A. Larrañaga, and J. M. Madariaga. 2019. "The Raman Spectra of the Na<sub>2</sub>SO<sub>4</sub>-K<sub>2</sub>SO<sub>4</sub> System: Applicability to Soluble Salts Studies in Built Heritage." *Journal of Raman Spectroscopy* 50: 175– 183. doi:10.1002/jrs.5550.
- Rodrigues, A., S. Fearn, T. Palomar, and M. Vilarigues. 2018. "Early Stages of Surface Alteration of Soda-Rich-Silicate Glasses in the Museum Environment." *Corrosion Science* 143: 362–375. doi:10.1016/j.corsci.2018.08.012.
- Sarmiento, A., M. Maguregui, I. Martinez-Arkarazo, M. Angulo, K. Castro, M. A. Olazábal, L. A. Fernández, et al. 2008. "Raman Spectroscopy as a Tool to Diagnose the Impacts of Combustion and Greenhouse Acid Gases on Properties of Built Heritage." *Journal of Raman Spectroscopy* 39: 1042–1049. doi:10.1002/jrs.1937.
- Schalm, O. 2000. *Characterization of Paint Layers in Stained-Glass Windows: Main Causes of the Degradation of Nineteenth Century Grisaille Paint Layers*. Antwerpen: Universiteit Antwerpen.
- Schalm, O., K. Janssens, and J. Caen. 2003. "Characterization of the Main Causes of Deterioration of Grisaille Paint Layers in 19th Century Stained-Glass Windows by J.-B. Capronnier." *Spectrochimica Acta Part B: Atomic Spectroscopy* 58: 589–607. doi:10.1016/S0584-8547(02)00282-3.
- Shantakumari, C. 1953. "Raman Spectra of Crystalline Sulphates of Zinc, Magnesium and Sodium." *Proceedings of the Indian Academy of Sciences - Section A* 37: 393–400. doi:10.1007/BF03052656.
- Silvestri, A., G. Molin, and V. Pomerio. 2011. "The Stained Glass Window of the Southern Transept of St. Anthony's Basilica (Padova, Italy): Study of Glasses and Grisaille Paint Layers." *Spectrochimica Acta Part B: Atomic Spectroscopy* 66: 81–87. doi:10.1016/j.sab.2010.11.015.
- Verità, M. 1996. "Composition, Structure et Mécanisme de Détérioration des Grisailles, Dossier de La Commission Royale Des Monuments." *Sites et Fouilles* 3: 61–59.
- Verità, M. 2010. "Paintwork in Medieval Stained-Glass Windows: Composition, Weathering, and Conservation." In *Proceedings of the Forum for the Conservation and Restoration of Stained Glass, The Art of Collaboration: Stained-Glass Conservation in the Twenty-First Century*, edited by M. B. Shepard, L. Piloni, and S. Stroble, 210–216. London: Harvey Miller.
- Verità, M., C. Nicola, and G. Sommariva. 2003. "The Stained Glass Windows of the Sainte Chapelle in Paris: Investigations on the Origin of the Loss of the Painted Work." *Annales du 16e Congrès de l'Association Internationale pour l'Histoire du Verre, Association Internationale pour l'Histoire du Verre Nottingham*, 347–351.
- Vilarigues, M., and R. C. Da Silva. 2004. "Ion Beam and Infrared Analysis of Medieval Stained Glass." *Applied Physics A* 79: 373–378. doi:10.1007/s00339-004-2538-9.

Vilarigues, M., and R. C. da Silva. 2006. "Characterization of Potash-Glass Corrosion in Aqueous Solution by ion Beam and IR Spectroscopy." *Journal of Non-Crystalline Solids* 352: 5368–5375. doi:10.1016/j.jnoncrysol.2006.08.032.

Vilarigues, M., C. Machado, A. Machado, M. Costa, L. C. Alves, I. P. Cardoso, and A. Ruivo. 2020. "Grisailles: Reconstruction and Characterization of Historical Recipes." *International Journal of Applied Glass Science* 11: 756–773. doi:10.1111/ijag.15793.

Vilarigues, M., P. Redol, A. Machado, P. A. Rodrigues, L. C. Alves, and R. C. Da Silva. 2011. "Corrosion of 15th and Early 16th Century Stained Glass from the Monastery of Batalha Studied with External ion Beam." *Materials Characterization* 62: 211–217. doi:10.1016/j.matchar.2010.12.001.